An integrated spectroscopic and wet chemical approach to investigate grass litter decomposition chemistry

Georgina A. McKee . Jennifer L. Soong . Francisco Calderon . Thomas Borch . M. Francesca Cotrufo

G. A. McKee, T. Borch, M. F. Cotrufo: Department of Soil and Crop Sciences, Colorado State University, Fort Collins, CO 80523, USA e-mail: mckee.georgina@gmail.com; J. L. Soong, M. F. Cotrufo: Natural Resource Ecology Laboratory, Colorado State University, Fort Collins, CO 80523, USA; F. Calderon: Agricultural Research Service, United States Department of Agriculture, Akron, CO 80526, USA; T. Borch: Department of Chemistry, Colorado State University, Fort Collins, CO 80523, USA; J. L. Soong: Department of Biology, University of Antwerp, 2610 Wilrijk, Belgium

Abstract

The chemical transformations that occur during litter decomposition are key processes for soil organic matter formation and terrestrial biogeochemistry; yet we still lack complete understanding of these chemical processes. Thus, we monitored the chemical composition of *Andropogon gerardii* (big bluestem grass) litter residue over a 36 month decomposition experiment in a prairie ecosystem using: traditional wet chemical fractionation based upon digestibility, solid state ^{13}C nuclear magnetic resonance (NMR) spectroscopy and Fourier transform infrared (FTIR) spectroscopy. The goals of this study were to (1) determine the chemical changes occurring during *A. gerardii* litter decomposition, and (2) compare the information obtained from each method to assess agreement. Overall, we observed a 97 % mass loss of the original litter, through a two-stage decomposition process. In the first stage, within 12 months, non-structural, cellulose and hemicellulose fractions not encrusted in lignin were preferentially and rapidly lost, while the acid unhydrolyzable residue (AUR) and microbial components increased. During the second stage, 12–36 months, all wet chemical fraction masses decreased equivalently and slowly with time, and the AUR and the lignin-encrusted cellulose fractions decomposition rates were comparable to each other. Method comparisons revealed that wet chemical fractionation did not accurately follow the initial litter structures, particularly lignin, likely because of chemical transformations and accumulation of microbial biomass. FTIR and NMR were able to determine bulk structural characteristics, and aid in elucidating chemical transformations but lacked the ability to measure absolute quantities of structural groups. As a result, we warn from the sole use of wet chemical methods, and strongly encourage coupling them with spectroscopic methods. Our results overall support the traditional chemical model of selective preservation of lignin, but shows that this is limited to the early stages of decomposition, while lignin is not selectively preserved at subsequent stages. Our study also provides important evidence regarding the impact of chemically different litter structures on decomposition rates and pathways.

Keywords: Litter decomposition, Cellulose, Hemicellulose, Lignin, NMR, FTIR, Grass, Big bluestem

Introduction

Plant residue (litter) decomposition is a key process assuring fundamental ecosystem functioning, such as the formation of soil organic matter and the cycling of nutrients. While we know that initial litter chemistry is a major factor controlling litter decomposition rates, and that litter with high nutrient concentrations and low lignin to cellulose ratios decompose faster (Aber et al. 1990; Talbot et al. 2011), there is an open debate regarding the chemical transformations that take place during decomposition. The conventional model is that litter decomposes through a stepwise process starting with the initial loss of soluble components, followed by the removal of labile moieties such as carbohydrates, while more recalcitrant compounds such as lignin are selectively preserved (Berg and McClaugherty 2007; Rovira and Rovira 2010). Many studies utilizing wet chemical approaches to identify litter chemical changes during decomposition support this hypothesis (Jung and Vogel 1992). More recently, studies using nuclear magnetic resonance (NMR) spectroscopy challenged this model of selective preservation of lignin, and proposed that lignin decomposes alongside other components (Lorenz et al. 2004; Preston et al. 2009), suggesting the importance of determining the chemical structural changes in order to accurately elucidate litter decomposition pathways (Buxton and Russell 1988; Jung and Vogel 1992; Soong et al. 2015; Cotrufo et al. 2015).

Traditionally, one of the most common methods to study litter decomposition has been wet chemical fractionation; dividing the litter into operationally defined moieties to identify key structural classes such as non-structural, cellulose, hemicellulose, tannins, and lignin (Van Soest and Wine 1968; Allen 1989; Rowland and Roberts 1994). These methods were originally developed to assess the quality of different feedstocks for animal nutrition (Van Soest et al. 1991). The main advantage of these methods is that they are quantitative and can be used to examine multiple types of litter under varying conditions (Hamadi et al. 2000; Sariyildiz and Anderson 2003). As a result, there is a large body of studies that generally support one another’s conclusions (e.g., Aber et al. 1990; Jung and Vogel 1992; Coûteaux et al. 1995; Hindrichsen et al. 2006; Sluiter et al. 2010). A major disadvantage of this method is that it does not provide any direct structural information since each fraction is operationally defined based on its resistance to sequentially stronger digests (Van Soest and Wine 1968).

Other commonly used methods to study litter decomposition are Fourier transform infrared (FTIR) and NMR spectroscopies (Lapierre 1993; Lorenz et al. 2004; Sjöberg et al. 2004; Preston et al. 2009; Xu et al. 2013; Bonanomi et al. 2013). The most notable advantage of these two methods is that they can examine ground litter without extraction (Nordén and Berg 1990; Smith 2011). Specific mid-infrared FTIR band absorbances can be used as

semiquantitative indices of organic matter functional group changes in litters (Calderón et al. 2006; Soong et al. 2014a). While diffuse reflectance FTIR does not conform strictly to the Beer–Lambert Law due to the unknown pathlength, previous studies show that the aliphatic CH, amide, aromatic, and polysaccharide-associated bands respond in a semi-quantitative fashion when adding standards to environmental samples (Calderón et al. 2013), and when using careful control of analytical conditions (Tremblay and Gagne 2002). Temporal changes in band intensities allow a determination of which chemical moieties are being lost or enriched upon decomposition of organic materials in soil (Mascarenhas et al. 2000; Calderón et al. 2006). In particular, FTIR spectroscopy has been valuable for the study of cellulose, hemicellulose and lignin because of the capacity to detect different C–O, aromatic C–H, and aromatic C=C bonds (Haberhauer and Gerzabek 1999; Nikonenko et al. 2005; Gorgulu et al. 2007). On the other hand, solid state NMR spectroscopy is able to examine the entire sample, but it is much less sensitive and so only bulk functional group classifications can be made (Lorenz et al. 2004; Sjöberg et al. 2004). Yet, semi-quantitative comparisons of ratios of broad structural groups in litter samples have revealed either few changes during decomposition (Preston et al. 2009) or enhancement in components considered to be recalcitrant (Bonanomi et al. 2013). The sensitivity of NMR can be significantly enhanced if isotopically enriched litter (e.g., ^{13}C and/or ^{15}N enriched) is examined with this method (Kelleher et al. 2006; Spence et al. 2011).

Combining multiple techniques to study litter chemistry maximizes their individual strengths and can significantly improve characterization and comparisons of litter samples at different stages of decomposition. We used this strategy in our study by combining wet chemical fractionation, FTIR and solid state ^{13}C NMR spectroscopy to examine the chemical composition of ^{13}C and ^{15}N isotopically enriched *Andropogon gerardii* (big bluestem; grass) sequentially as it decomposed on the soil surface in a tall grass prairie over a 3 year timeframe. Big bluestem is the major grass species dominating the Midwestern states (Jung and Vogel 1992; Zhang et al. 2012) and its decomposition plays a vital role in recycling nutrients and building soil organic matter in prairie ecosystems. The goals of our study were to (i) determine the chemical changes in above ground *A. gerardii* litter residue as it sequentially decomposed and (ii) compare the information and agreement obtained from three analytical techniques to measure these changes.

Materials and Methods

Study site

The litter decomposition experiment was conducted at the Konza Prairie biological research station in Kansas, USA (39.0931 °N, 96.5586 °W). It is a tallgrass prairie ecosystem dominated by *A. gerardii*. Climate at the site is temperate-continental, with a mean annual temperature of 12.8 °C and average annual precipitation of 835 mm. The soil is a silty clay Mollisol with

approximately 4 % C and 0.32 % N, and presents characteristics of the footslope soils at the site (Knapp et al. 1998). The site is locally referred to as the R20B watershed.

Litter decomposition

In June 2010 we installed 20 cm diameter PVC collars at the site to a depth of 5 cm. We removed the native litter layer from within the collars and applied 4 ml of glyphosate to deter plant growth within the collars. The litter decomposition experiment began on September 29, 2010 (month 0/initial), when 18.4 g of ^{13}C and ^{15}N labeled *A. gerardii* litter was placed on the soil surface within the collars. Litter addition corresponded to an estimated local above ground net primary production of 400 g/m^2 (Knapp et al. 1998). The isotopically labeled litter used throughout the experiment (3.4 at. % ^{13}C and 4.0 at. % ^{15}N) was produced in a continuous isotope labeling chamber in the laboratory as described by (Soong et al. 2014b). The litter was approximately 21 weeks old when leaves and stalks were harvested for this experiment, and was showing initial signs of senescing (% C—44.3 and % N—1.47). A full description of the litter decomposition experiment is provided in (Cotrufo et al. 2015).

Briefly, it consisted of a fully randomized complete block design with 4 replicate blocks. Within each replicate block, five whole plots each with a PVC collar were randomly assigned to one of the five sampling dates. On May 1 2011 (6 months), October 8, 2011 (12 months), April 14 2012 (18 months), September 29, 2012 (24 months), and September 25, 2013 (36 months; at which point it was determined there was not enough material left to continue), all visible litter residues remaining on the soil surface were collected by tweezers from within collars in each of the four replicate plots. The litter was stored in plastic bags at 5 °C. Within two days of collection, the litter was picked clean of any non *A. gerardii* leaves, roots, and soil, and weighed at field moisture. A subsample of the initial litter and of each litter after collection from the field was oven dried at 65 °C for analysis of gravimetric water content, and another subsample was combusted at 660 °C in a muffle oven to determine ash content. The litter samples were then ground and analyzed by wet chemistry, FTIR, and NMR. Total litter mass loss was determined on an ash-free dry mass base as the difference between the initial mass and that at month 36 and expressed in percent of the initial. Isotopic analyses of the litter through time revealed that exogenous C and N were incorporated in the litter residues, likely through fungal hyphae growth, but exogenous inputs were only significant (ca. 30 % of the total) for N between month 6 and 24 (Soong et al. 2016).

Wet chemical analyses of the litter

Proximate estimates of cellulose and acid unhydrolyzable residue (AUR, commonly referred to as lignin) content were measured using an Acid Detergent Fiber (ADF) (Van Soest and Wine 1968) method on the litters from 0, 6, 12, 18, and 24 month harvests. Briefly, an initial heated digestion in

cetyl trimethylammonium bromide (CTAB) and sulfuric acid removed hemicellulose and other non-structural carbohydrates and lipids, what remained were α-cellulose, AUR, and ash. The sample was then digested in 73 % sulfuric acid to digest the α-cellulose. The final AUR fraction was combusted at 660 °C to determine ash content. The fractions were ash corrected and calculated gravimetrically (mass precision = 0.00001 g, except initial litter − mass precision of 0.01 g) and were thus proximate estimates for α-cellulose (referred to as cellulose from hereon) and AUR (Rowland and Roberts 1994). Non-structural material and hemicellulose content was determined by difference using the Neutral Detergent Fiber (NDF) method (Van Soest et al. 1991) on different litter subsamples of the same time harvests as above. The NDF digested the non-structural plant material and left behind hemicellulose, cellulose, and AUR. The hemicellulose content was calculated as the difference between the NDF insoluble fraction and the ADF fraction. At 36 months, not enough litter mass remained for the ADF and NDF digestions.

It is important to note that the wet chemical fractionation method is operationally defined and based on the approach of dividing the litter into fractions based on their ease of digestion by ruminants (Van Soest and Wine 1967, 1968). The non-structural pool of the litter is composed of the cellular material, which includes organic acids, sugars, starches and fructans, and proteins (Ishler and Varga 2001). It is generally considered to be the most bioavailable fraction of the litter and most easily digestible by microbes. The cellulose (α-cellulose) fraction is thought to represent all of the cellulose that is naturally present in the plant walls (Davies et al. 2002). Likewise, the hemicellulose fraction is assumed to contain all hemicellulosic material in the plant walls (Van Soest and Wine 1968). The AUR fraction is usually considered to be primarily composed of lignin (Sluiter et al. 2010); although this has been disputed (Preston et al. 2009). For each litter fraction, its change over time was calculated by subtracting its mass at each harvest from the corresponding initial fraction mass for each field replicate (n = 4) and reported in percent change from the initial fraction mass.

Fourier transform infrared spectroscopy

The dried and ground litter samples of the 0, 12, 24, and 36 month litter were scanned from 4000 to 400 cm^{-1} using a Digilab FTS 7000 infrared spectrometer (Varian, Inc., Palo Alto, CA) with a deuterated triglycine sulfate detector and a (KBr) beam splitter. The instrument was fitted with a Pike AutoDIFF diffuse reflectance autosampler (Pike Technologies, Madison, WI). KBr was used as a background. Data were recorded as pseudo absorbance (log [1/Reflectance]), with 4 cm^{-1} resolution, and 64 scans were co added per spectrum. Spectral averages and spectral subtractions were carried out using GRAMS Al version 9.1 software (Thermo Fisher, Woburn, MA). The Spectral Subtract (SUBTRACT.AB) application of GRAMS/Al 9.0 was used to perform the subtractions. The GRAMS/Al feature uses the dewiggle algorithm described by (Banerjee and Li 1991). We used the optimal factor and

tolerance values suggested by the software. Mid IR spectra contain fundamental and overtone bands of functionalities that sometimes overlap, which complicates the spectral interpretation. Second derivatives allow for specific identification of peaks that are too close to each other to be observed clearly in the original spectrum (Whitbeck 1981), details of the derivitization are included in statistical tests below.

Solid state ^{13}C nuclear magnetic resonance spectroscopy

Dried and ground litter samples of the litter from 0, 12, 24, and 36 months were utilized for all NMR analyses. A 500 MHz Varian spectrometer operating at 125 MHz resonance for ^{13}C and 500 MHz resonance for ^{1}H equipped with a 4 mm multi nuclear probe spectrometer housed at the Environmental and Molecular Science Laboratory (EMSL) at Pacific Northwest National Laboratory was used for all studies. A one dimensional solid state cross polarization magic angle spinning (CPMAS) pulse sequence (^{13}C–^{1}H) was engaged for all samples. The pulse sequence utilized a ramped pulse on the proton applied for 4 μs before transference to the ^{13}C using a 1 ms contact time. The recycle delay between pulses was 4–8 s; optimized for each sample. It should be noted that CPMAS generally under represents aromatic species due to the longer distance between C and H. However, we do not anticipate severe issues, since the aromatic content of *A. gerardii* is low (Theerarattananoon et al. 2012). Samples were packed in Kel-F rotors with approximately 80–90 mg. Samples were spun at 14 kHz at the magic angle, with no noticeable spinning sidebands in the region of scanning (0–300 ppm). 500 data points were acquired for each sample. Each sample was 100 Hz line broadened, apodized, phased, calibrated using hexamethyl benzene, and baseline corrected prior to integration. Integration regions were distinguished based on an earlier assignment of regions for *A. gerardii* and other studies of cellulose and lignin spectra (Vanderhart and Atalla 1984; Theerarattananoon et al. 2012). Integration ratios (the percent of signal per region/structural group) were calculated by summing all integration values for the whole spectrum and dividing it by the individual regions, to obtain integration ratios based upon the change within each sample. Although this method is semi quantitative and does not relate to the concentration of each region in the sample, it did allow us to compare and contrast samples throughout the experiment, observing changes and continuities. A number of decomposition indexes have been developed to help examine litter by NMR spectroscopy (Bonanomi et al. 2013). We applied the same decomposition indexes (or integration ratios) to our spectra to assess quantitatively if any could shed more light upon the decomposition process as measured by NMR.

Statistical analysis

The FTIR spectra were derivatized using the second derivative and a gap of 18.015 using GRAMS AI 9.1. The second derivatives have the added advantage of preventing baseline artifacts. Note that derivatization converts positive peaks in the FTIR spectrum into negative peaks, so a negative R

score actually denotes a positive correlation. Pearson correlation coefficients of FTIR spectral bands and wet chemical data were calculated using GRAMS IQ version 9.1 software (Thermo Fisher, Woburn, MA).

Linear regression analyses ($\alpha = 0.05$) were performed on plots of decomposition indexes (or integration ratios) with time (month) for both NMR and wet chemical data (Supplementary Fig. 1). Details of the tests performed on each data set to validate the statistical analyses are included in the Supplementary Text.

Results

Initial (month 0) litter chemical composition

Wet chemical fractionation

As determined by wet chemical analysis (operationally defined) (Table 1), the *A. gerardii* above ground litter was primarily composed of non-structural components (42 %). Cellulose and hemicellulose fractions were the second (29 %) and third (25 %) largest recovered. The AUR fraction was a very small component of the litter (4 %).

Table 1 Masses of remaining total litter and litter chemical constituents as analyzed by wet chemical digestions

Month	Field mass (g)	Non-structural (g)	Hemicellulose (g)	Cellulose (g)	AUR (g)	Ash (g)
0	18.4	7.7353	4.6218	5.2718	0.7230	0.0482
6	12.6313 (1.270)	3.2651 (0.361)	3.1089 (0.232)	4.0490 (0.367)	1.2673 (0.165)	0.9409 (0.203)
12	6.21871 (0.212)	1.8968 (0.123)	0.9520 (0.013)	1.8082 (0.057)	1.0148 (0.074)	0.5153 (0.060)
18	5.0279 (0.392)	1.6722 (0.163)	0.7211 (0.054)	1.3221 (0.146)	0.8180 (0.058)	0.4944 (0.022)
24	4.0760 (0.496)	1.0680 (0.187)	0.6144 (0.192)	0.8418 (0.172)	0.6913 (0.111)	0.8603 (0.140)
36	0.4950 (0.150)	NA	NA	NA	NA	NA

Data are averages with standard error in parentheses ($n = 4$), except for the initial litter which had no replicates. The field mass is the ash corrected dry mass remaining

NA not enough available to conduct chemical analyses

FTIR analysis

The FTIR analysis of the initial litter spectra had the expected bands assigned to O–H/N–H stretching at 3400 cm^{-1}, the aliphatic C–H bands at 2950–2860 cm^{-1}, as well as the ester carbonyl band from polysaccharides or fatty acids at 1735 cm^{-1} (Fig. 1). Besides these bands, two peaks with possible aromatic absorbance are observed within the fingerprint region, namely 1610 and 1510 cm^{-1}. The small shoulder at 1464 cm^{-1} could be assigned to cellulose C–H deformation. The small peak at 1427 cm^{-1} is assigned to C–H in cellulose, hemicelluloses, or lignin. The bands at 1373 and 1319 cm^{-1} are due to the CH_2 in cellulose and hemicelluloses. The region between 1150–1060 cm^{-1} contains bands that can be assigned to several macromolecules, including lignin or cutin (C–O and C–O–C stretch), and/or polysaccharides such as cellulose.

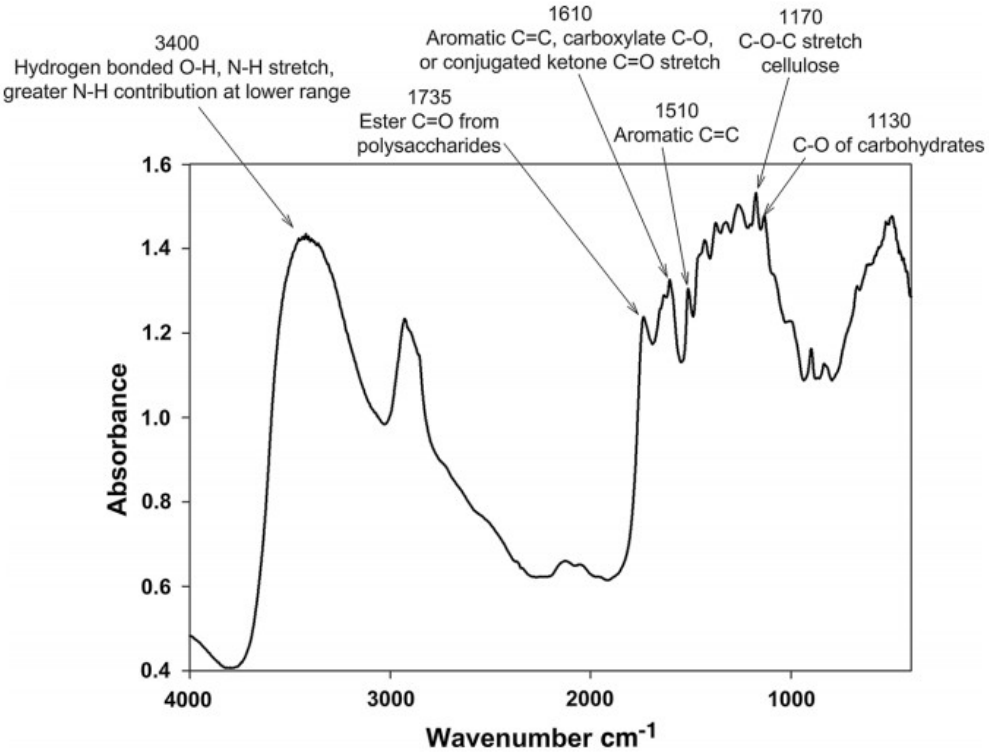

Fig. 1 Big Bluestem initial litter FTIR spectrum

NMR analysis

The solid state ^{13}C NMR spectrum (Fig. 2) of the initial litter was composed of a mixture of lignin, cellulose, hemicellulose, and protein; as found from the wet chemical and FTIR results. The dominant structural group was the C2, C3 and C5 of the cellulose structure (67–80 ppm), which is logical considering the greater number of carbon atoms contributing to it, and the high content of cellulose in the initial litter indicated by the wet chemical analysis. The C6 cellulose region was the next most dominant (59–67 ppm), followed by the C1 cellulose peak (94–113 ppm). Overall and consistent with the wet chemical analysis, cellulose was the dominant structural group of the NMR spectrum.

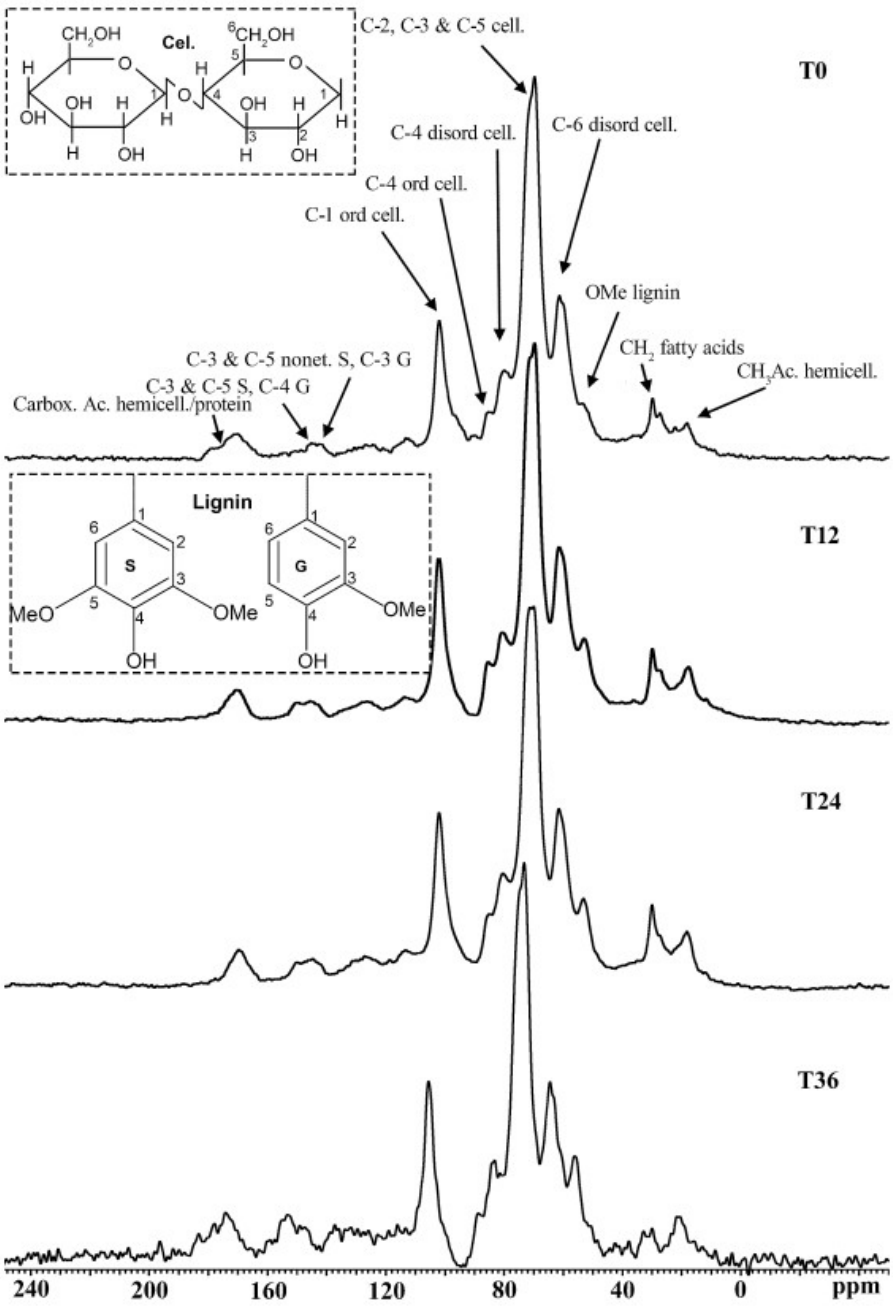

Fig. 2 ^{13}C solid state NMR spectra by time (months). Example structures for cellulose and lignin monomers are displayed and their carbon numbers are identified in the NMR spectrum. *cel.* is cellulose, *hemicel.* hemicellulose, *dis.* disordered, *ord.* ordered, *nonet.* noneteried, *Carbox.* carboxyl, *Ac.* acetyl, *G* guaiacyl, *S* syringyl

Hemicellulose regions were the next most dominant in the initial litter, particularly the methyl group of hemicellulose's acetyl (0–25 ppm). The 161–181 ppm region was partially composed of the acetyl group in hemicellulose and a region from carboxyl carbon in proteins (Himmelsbach et al. 1983). The methoxy group of lignin was the most dominant lignin region, as expected, since all lignin monomers contribute to this region (46–59 ppm). The two other lignin regions in the spectrum were both relatively small (143–150 and 150–161 ppm). The etherified and non-etherified regions of the spectrum could indicate possible strong crosslinks often observed between lignin and arabinoxylans (components of hemicellulose), especially for

mature plants such as the one in our study (Casler and Jung 1999, 2006). More detailed region assignments were not possible due to the overlap of multiple groups in chemical shift regions.

Changes in litter during decomposition

Mass loss

The largest mass loss of litter was observed during 0–12 months of decomposition (Table 1), when two thirds of the litter was lost. Between 12–24 months, there was a less dramatic change in mass, with only one third of the litter being lost. From 24 to 36 months, only 10 % of the remaining litter was lost compared to the 24 month harvest. By the end of the 36 months of decomposition 97 % of the initial litter mass was lost. Decomposition pathways and the fate of litter C and N during decomposition are described in (Cotrufo et al. 2015).

Wet chemical fractionation

The compositional makeup (as measured by wet chemistry) of the remaining litter for each harvest changed as decomposition proceeded (Table 1). By month 6, we observed a preferential loss of non-structural compounds whose content dropped by 58 % (Fig. 3a). Also cellulose and hemicellulose components decreased at a similar rate (23 and 33 %, respectively) while the AUR increased by 75 % (Fig. 3a; Table 1). In terms of relative concentrations, these changes resulted in a leveling out of the non-structural, cellulose and hemicellulose fractions to about 25–30 % while the AUR reached about 10 % of the litter. The period between 6 and 12 months was characterized by a parallel loss of the cellulose and AUR fractions (Fig. 3a; Table 1). By 12 months, the litter residue had a non-structural and cellulose amount of approximately 30 %, and a hemicellulose and AUR concentration of around 15 % each. The composition did not vary considerably from 12–24 months, when the litter appeared to lose mostly AUR (Fig. 3a).

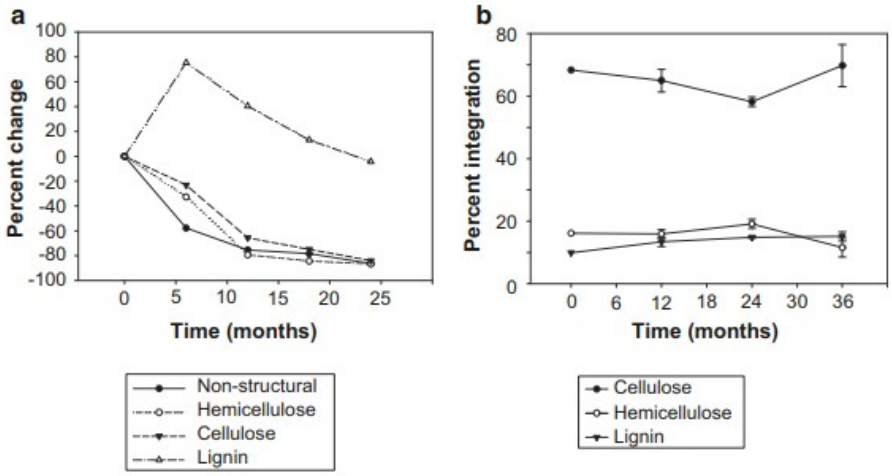

Fig. 3 Chemical changes during big bluestem decomposition, as **a** percent change by month for wet chemical fractions and **b** total solid state ^{13}C NMR integration percentages by general structural class for each harvest and initial litter. Harvest litters are the average of two NMR spectra

FTIR subtractive analysis and correlation with wet chemical data

Spectral changes during decomposition were relatively small and best shown by the subtractive spectra for two time intervals: 0–12 months of decomposition, and 12–36 months. Downward peaks in the subtraction spectra denote bands that increased during the respective periods. For the first time interval (from 0 to 12 months) we observed marked changes in the FTIR spectra of the litter (Fig. 4). Absorbance at the broad O–H/N–H stretching around 3355 cm^{-1} increased with decomposition. This band was prominent in the spectra of both pure cellulose and lignin (Reeves et al. 2008). However, the cellulose content of the litter as assessed by wet chemistry and NMR decreased during this period (Fig. 3a, b). This suggests that the increased absorbance at 3400 cm^{-1} was due to the increased concentration of –OH containing materials other than cellulose, such as microbial biomass, and non-cellulose polymers during the first 12 months of decomposition (Fig. 4). The absorbance at 2925–2850 cm^{-1} (aliphatic C–H) also increased during the first 12 months. Gains in absorbance at 1675 and 1540 cm^{-1} suggested an increase in proteins or amides. Absorbance between 1170–1000 cm^{-1}, centered at 1080 cm^{-1} (C–O and C–O–C stretch, and Si–O) also increased markedly during the first 12 months.

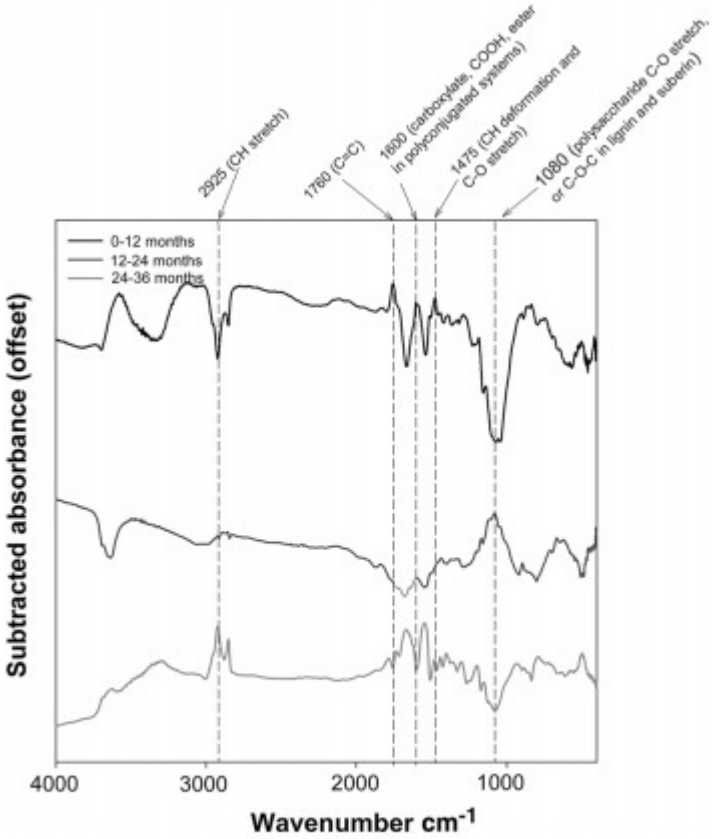

Fig. 4 FTIR spectral subtractions for each 12-month interval. The absorbance data was offset to stack the different spectra and aid visualization

Between 12 and 36 months, the differences shown by the FTIR subtractions were more subtle than in the first 12 months (Fig. 4). The litter mass losses observed during this period (12–36 months) were less than the first 12 month period (Table 1). Spectral changes at 3400 and 2925–2850 cm^{-1} were opposite to the 0–12 month interval (Fig. 4). There were losses in absorbance at 2925–2850 cm^{-1}. Increased absorbance at 1500 and 1610 cm^{-1} indicated an increase in concentration of lignin in the decomposing litter in the last 24 months of decomposition. Spectral subtraction shows that between 12 and 24 months of decomposition, lattice clays were incorporated into the decomposing residues as indicated by an increase in absorbance at 3695 cm^{-1}.

The subtraction of the initial litter spectrum from the 36 month spectrum showed that the most marked spectral changes were a net increase in the 1670, 1540, 1510, and 1230 cm^{-1} bands (not shown). This was indicative of lignin and polyconjugated systems. There was also a large net increase in the band between 1100–1030 cm^{-1}; which was accompanied by a small increase at 3695 cm^{-1}.

The correlation analysis between the derivatized FTIR data and the wet chemical data showed several bands that increased with AUR over the first 24 months of the study: 2930, 2853, 1740, 1670, 1655, 1545, 1464, 1155, and 926 cm^{-1} (Table 2). Yet, only bands near 1512, and 1601 cm^{-1} have been attributed to lignin in the literature (Xu et al. 2013). Our results showed that as the AUR became concentrated in the decomposing litter over the 3 year period, absorbance in these two bands decreased (Table 2). However, if only the time between months 12 and 36 was taken into account, the lignin bands at 1512 and 1601 cm^{-1} increased, corresponding to the AUR fraction changes (Fig. 3). Correlation results were similar for cellulose and hemicellulose (Table 2). Bands correlated with cellulose and hemicellulose content were 897, 1126, 1173, 1319, 1512, and 1601 cm^{-1}. The non-structural fraction had correlation coefficients below 0.5 for all the selected spectral bands.

Table 2 Pearson correlation coefficients between the derivatized FTIR data and the wet chemical data for the first 2 years of the litter decomposition experiment (n = 17)

FTIR data		Wet chemical fractions			
Absorbance (cm^{-1})	Assigned functionalities	AUR/lignin	Cellulose	Hemicellulose	Non-structural
897	Cellulose	0.60	−0.78	−0.67	0.23
926	Cellulose, hemicel	−0.41	0.79	0.53	−0.31
1126	Cellulose, hemicel, lignin	0.75	−0.68	−0.74	0.18
1155	C–O stretch of proteins and carbohydrates	−0.80	0.55	0.78	0.01
1173	Cellulose, hemicel	0.73	−0.73	−0.67	0.12
1319	Cellulose, hemicel	0.32	−0.70	−0.36	0.34
1373	Cellulose, hemicel	0.10	−0.36	−0.32	0.42
1427	Cellulose, hemicel, lignin	−0.07	−0.29	−0.08	0.34
1464	Cellulose	−0.58	0.20	0.38	0.01
1512	Lignin	0.48	−0.40	−0.54	−0.16
1545	N–H bend and C=N stretch (amide II)	−0.66	0.29	0.68	0.11
1601	Lignin	0.66	−0.46	−0.66	−0.14
1655	Lignin	−0.45	−0.16	0.08	0.36
1670	C=O stretch and/or amide I	−0.77	0.43	0.70	0.11
1740	Hemicel	−0.55	0.42	0.31	−0.02
2853	Lignin	−0.55	0.10	0.52	0.02
2930	Lignin	−0.43	−0.03	0.44	−0.01

Band assignments in the footnote are from Xu et al. (2013) and Theerarattananoon et al. (2012). Due to the second derivative treatment of the spectral data, negative coefficient values indicated a positive proportional relationship, while positive values indicated a negative inversely proportional relationship. C–H stretching band = 2930 and 2853 cm^{-1}, C=O ester strong in branched hemicellulose = 1740 cm^{-1}, amide or lignin = 1655 cm^{-1}, lignin aromatic skeletal vibration or C=O stretching = 1601 cm^{-1}, lignin C=C = 1512 cm^{-1}, cellulose C–H deformation = 1464 cm^{-1},C–H bend in cellulose, hemicelluloses, lignin = 1427 cm^{-1}, CH_2 wag in cellulose and hemicelluloses = 1373 cm^{-1}, CH_2 wag in cellulose and hemicelluloses = 1319 cm^{-1}, C–O–C asymmetrical in cellulose and hemicelluloses = 1173 cm^{-1}, cellulose, hemicelluloses or lignin various functionalities = 1126 cm^{-1}, and cellulose antisymmetric out-of-plane ring stretch = 897 cm^{-1}

Structural group NMR analysis

The relative contributions to the NMR signal for the different harvests for the three major groups (cellulose, hemicellulose, and lignin) in the litter (Figs. 3b, 5; Table 3) showed that, throughout decomposition, cellulose regions

dominated the litter. Some of the cellulose regions (59–67, and 67–80 ppm regions), showed dramatic decreases in relative abundance for the first 12 months, and by 24 months the relative abundance for all cellulose groups (59–67, 67–80, 80–87, 87–92 and 94–113 ppm regions) had decreased. Whereas all of the cellulose regions had increased in relative abundance after 36 months; returning to a similar level as in the initial litter (Fig. 3b). For all of the lignin assigned regions, we saw an increase in methoxy lignin especially between 0 and 24 months; suggesting a relative preferential preservation for this traditionally considered recalcitrant structure during the early stages of decomposition (Fig. 5). In the 36 month sample we observed the methoxy lignin peak (46–59 ppm) was at its highest with a smaller incremental change from the earlier harvest (24 month), other lignin peaks had more subtle changes. The hemicellulose regions (0–25 and 161–181 ppm regions) generally slightly increased for the 12 and 24 month samples compared to the initial litter. However, the methyl group in the acetyl of hemicelluloses (0–25 ppm) was dramatically lower in the 36 month sample compared to any of the earlier samples (Fig. 5).

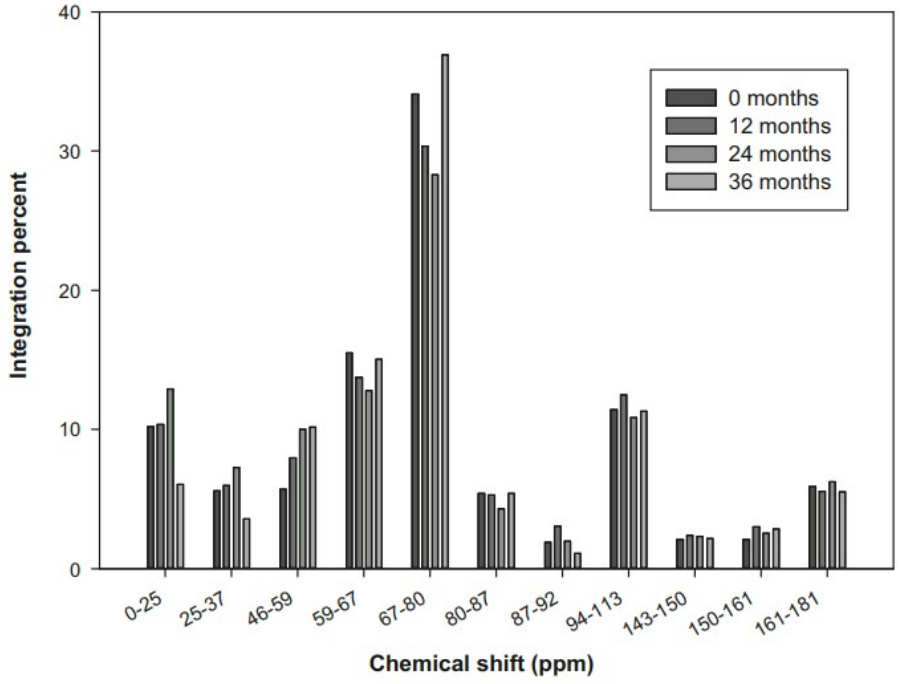

Fig. 5 Relative integration percentages (averaged for months 12–36) of each chemical shift region by month. Structures assigned to chemical shift regions are displayed in Table 3

Table 3 Integration regions assigned to structural classes as determined by NMR spectroscopy for big bluestem litter spectra in Fig. 5

Integration region (ppm)	Structural class
0–25	Methyl of acetyl in hemicellulose
25–37	Methylene
46–59	Methoxy lignin
59–67	C-6 crystalline/amorphous cellulose
67–80	C-2, C-3 and C-5 cellulose
80–87	C-4 disordered amorphous cellulose
87–92	C-4 ordered crystalline cellulose
94–113	C-1 cellulose
143–150	Nonetherified C-3 & C-5 syringyl, C-3 guaiacyl
150–161	Etherified C-3 & C-5 syringyl, C-4 guaiacyl
161–181	Carboxyl of acetyl hemicellulose/protein

Of the decomposition indexes we compared, the most effective ratios were the O-alkyl (60–90 ppm) to methoxy in lignin (45–60 ppm) ratio and C2, C3 and C5 from cellulose (67–80 ppm) to methoxy in lignin (46–59 ppm) ratios, both decreased with decomposition time. The ratios which included a measure of the relationship of either the aromatic region of the spectrum with alkyl groups or the O-alkyl region to the alkyl region did not show any change with time.

Although the differences in the chemical composition derived by NMR were more subtle they generally supported the wet chemical fractionation data. To illustrate the two step decomposition process we observed, we sought to link the subtle NMR changes with the wet chemical fractions. We plotted the cellulose/AUR ratio against time in two graphs, split by time (0–12 and 12–24 months) for the wet chemical data. We made the same plot for the NMR data (C2, C3, C5 cellulose to methoxy lignin region ratio) but were unable to split the time axis into the two steps due to a lack of data points. The NMR plot indicated a decreasing linear relationship with time (Supplementary Fig. 1a, $R^2 = 0.773$, $\alpha = 0.05$, $p = 0.496$), however, the low probable confidence of this relationship and the low number of data points (an average of 500 separate analyses per sample) mean that this trend only demonstrated a likely relationship. For the wet chemical plot we reported a high R^2 value for the 0–12 month plot (Supplementary Fig. 1b, $R^2 = 0.843$, $\alpha = 0.05$, $p = 0.000475$), with a relatively steep slope of −0.38. This correlated to a preferential loss of cellulose in contrast to the unchanging AUR content over time (0–12 months). The 12–24 month plot (Supplementary Fig. 1c) effectively illustrated that cellulose was no longer being preferentially lost compared to the AUR fraction.

Discussion

Initial litter (Month 0) chemical composition

Overall, the values obtained for the different ADF and NDF fractions using wet chemical fractionation of big bluestem in this study resulted in similar fraction amounts to other warm season grasses including switchgrass and

big bluestem (Jung and Vogel 1992). The initial NMR analysis (Fig. 2) of big bluestem was also in agreement with previous studies for big bluestem (Theerarattananoon et al. 2012), and other grasses (Nelson and Baldock 2005; Preston et al. 2009; Bonanomi et al. 2013), likewise for the FTIR data (Theerarattananoon et al. 2012).

It is important to recognize that NMR is unable to differentiate between structural and non-structural carbohydrates (Lewis et al. 1988). This made it challenging to compare the cellulose results for each method (Fig. 3). Comparing total hemicellulose fractions, NMR indicated approximately 16 % hemicellulose whilst the wet chemical analysis indicated 25 %. The wet chemical hemicellulose amount was similar to other wet chemical method studies (Zhang et al. 2012) but it could be an over estimate due to silica inclusion (Udén et al. 2005), or the incorporation of noncore lignin (Dann et al. 2006). NMR did not have these possible interferences and so it was likely to be a more accurate determination of the hemicellulosic content. Despite this difference, both methods indicated that hemicellulose is of secondary importance to cellulose. Further, FTIR investigation of the C1 peak indicated that it was a singlet peak (Fig. 1), suggesting that the dominant cellulose type for the initial litter was cellulose I (Davies et al. 2002).

The AUR fraction was the smallest for both wet chemical fractionation and NMR, albeit their percentages varied, 4 and 10 %, respectively. Based solely on these percentages, and comparing those values to previous studies on big bluestem, the wet chemical fractionation method appeared to be underestimating the amount of lignin present in our litter (the AUR fraction). The AUR in this study was in agreement with previous lignin estimates for big bluestem (3.9 % using a sequentially determined acid detergent lignin method) (Goff et al. 2012) but in contrast with others (17 % lignin using National Renewable Energy Laboratory analytical procedures) (Zhang et al. 2012). There were several possible reasons for why the total amount of lignin (thought to be in the AUR fraction) was likely underestimated (Goff et al. 2012). Firstly, the noncore lignin (monomeric phenolic acids esterified to phenolic compounds) in the ADF could have been under represented (due to lack of access), consequently increasing the apparent amount of the non-structural fraction (Jung and Vogel 1992; Dann et al. 2006). Secondly, the incorporation of other structures such as tannins and cutin within the AUR has been found to be a particular problem for some litters (Preston et al. 1997).

Despite the problem of unequivocal FTIR assignment of lignin bands such as assigning 1060–1150 cm^{-1} to either (1) ether C–O–C absorbance from lignin (Socrates 1994), (2) polysaccharide absorbance (Stewart et al. 1995), or (3) C–O and C–O–C stretching in suberin or cutin, the band at 1515 cm^{-1} (C–H deformation and aromatic skeletal vibration) and at 1610 cm^{-1} (aromatic C=C vibration) were perhaps the most unequivocally assigned to lignin, and both were observed in the spectrum of initial litter (Fig. 1).

Stage 1 of decomposition: 0–12 months

The changes we observed during the course of the decomposition by wet chemical fractionation were generally similar to other studies (Coûteaux et al. 1995; Adair et al. 2008). Between 60–80 % of the original mass of the non-structural, hemicellulose, and cellulose fractions were lost by month 12 (Fig. 3a). We observed in the NMR spectra that the majority of the cellulose regions decreased, while hemicellulose regions did not, suggesting that cellulose was selectively removed to some extent (Fig. 5).

FTIR bands that declined during the first 12 months included primarily labile functionalities at 1760 cm^{-1} (lipid C=C, or ester group C=O vibration in triglycerides or hemicellulose), 1600 cm^{-1} (lignin aromatic skeletal vibration (Theerarattananoon et al. 2012), but more likely in our case C=O stretching due to low AUR), and 1475 cm^{-1} (cellulose C–H deformation). Overall, the dynamics of the FTIR spectra were consistent with a net loss of carbonyl-rich molecules such as polysaccharides.

FTIR data also revealed that the aliphatic C–H became concentrated due to the disappearance of more labile C moieties (Fig. 4). This could have been because; (1) other less labile, aliphatic-rich molecules such as cutin and suberin could have been a significant component of plant litter C (Rumpel et al. 2004; Spielvogel et al. 2010), (2) cell wall components rich in aliphatic character could have been a component of the AUR (Preston et al. 1997), which increased (Figs. 2, 3). The methylene region in the NMR spectra (25–37 ppm) increased, likely due to waxes (Nordén and Berg 1990). We noted however, that the aliphatic C–H bands between 2950–2860 cm^{-1} had some assignment discrepancy in previous studies of carbohydrates (Theerarattananoon et al. 2012) and lignin (Xu et al. 2013). Plant derived and/or soil minerals had an effect on the FTIR spectral changes that occurred in the different stages of the incubation. The strongest Si–O stretching vibrations in silicate spectra occurred between 1100–900 cm^{-1}, while clay associated silicates had O–H stretching vibration bands from 3700 to 3620 cm^{-1} (Madejová et al. 2002). Between 0–12 months the increased absorbance around 1080 cm^{-1} could have been in part explained by the increased concentration of Si–O originally present in the plants.

The biggest change as determined by wet chemical fractionation was observed in the AUR fraction (Fig. 3), which increased by almost 80 % within the first 6 months, similar to previous observations (Hamadi et al. 2000; Preston et al. 2009). Consistently, during this early period we observed an increase in the FTIR absorbance at 1120–1020 cm^{-1} (Fig. 4) which could be derived from a number of structures such as lignin (Socrates 1994), polysaccharides, or from suberin/cutin (Stewart et al. 1995). A possible explanation for those increases in the wet chemical AUR fraction could have been the formation of lignin-polysaccharide structures as a result of microbial activity (Cortez et al. 1996; Hamadi et al. 2000). We observed visible fungal colonies growing on the litter during the course of

decomposition, for which we saw direct spectroscopic evidence from the increasing FTIR absorbances at 1660 and 1540 cm^{-1} (Fig. 4). The absorbances could have been due to microbial protein amide I (C=O stretching vibration, 1660 cm^{-1}), and amide II absorbance (N–H bending/C–N stretching vibrations, 1540 cm^{-1}); similar to Klaison lignin (Preston et al. 1997). In traditional models, lignin is thought to be stable during the early stages of litter mass loss (Berg and Staaf 1980). However, a new model proposed by (Klotzbücher et al. 2011), suggested that bioavailable C is necessary for the removal of lignin, and therefore, lignin is initially removed quickly, but then removal slows down as C bioavailability decreases. Our study did not support the Klotzbücher et al. model, instead it suggested an accumulation of the AUR fraction, and the preferential losses of water soluble and free cellulose in the early stages of decomposition.

Despite the extensive mass loss with decomposition time (Table 1), and the strong decrease in the most labile fractions of the wet chemical fractions with time (Fig. 3a) we did not observe dramatic changes in the NMR spectra (Fig. 5), which is in agreement with previous studies (Preston et al. 2009). The process of litter decomposition appeared to render fractions of the original litter insoluble (Kolodziejski et al. 1982; Talbot et al. 2011), likely because of subtle alterations in the chemical structure impacting their solubility such as by the formation of cellulose-lignin structures (Supplementary Fig. 1), leading to a no net change in the bulk functional groups present in the litter. The addition of microbial matter (Kögel-Knabner 2002) to the litter could also have led to less observable changes (Fig. 4).

Stage 2 of decomposition: 12–36 months

We observed a 97 % mass loss, that indicated full mass loss over the 36 months we conducted this experiment. However, Cotrufo et al. 2015 indicated that the investigated litter residues were also physically mobilized to the underlying soil between month 12 and 36, thus the amount of litter originally placed on the soil surface did not only decrease due to mineralization but also due to physical mass transport and leaching.

The strong correlations between FTIR spectral bands and the wet chemistry fractions for cellulose and hemicellulose (Table 2); especially 897, 1126, 1173, and 1319 cm^{-1} (Theerarattananoon et al. 2012; Xu et al. 2013) suggested that these bands could be used to monitor cellulose/hemicellulose dynamics in decomposing litter.

There was however a disparity between NMR and the other two methods for some cellulose and hemicellulose region/component changes. For example, the hemicellulose regions in the 24 month sample increased as measured by NMR (Fig. 5), opposite to the trend measured by wet chemistry (Fig. 3a); however by month 36, we noted a decreasing trend for hemicellulose from both methods. In contrast, some of the FTIR absorbances that could have been assigned to cellulose (897 and 1464 cm^{-1}) and hemicellulose (1740 cm^{-1}) both increased, while others such as 1050–1130 and 3400 cm^{-1},

remained constant. A possible reason for this apparent disparity could be because the absorbances for cellulose and hemicellulose were quite similar and multiple absorbances can be assigned to polysaccharides to produce apparent differences in trend with time.

From month 12 to 24 the size of the AUR fraction decreased, suggesting it was decomposed or reallocated to a different fraction during this later stage (Fig. 3a) (Berg and Staaf 1980; Klotzbücher et al. 2011). We observed a similar loss in the methoxy lignin region (46–59 ppm) (Fig. 5; Table 3). However, there was a lack of change in the non-etherified syringyl (143–150 ppm) region suggesting it could be recalcitrant or insoluble (such as certain lignin monomers). The FTIR data showed a net increase in lignin-associated bands, as well as the inclusion of minerals (Nguyen et al. 1991). For example, the absorbances at 2930–2850, 1670, and 1545 cm^{-1} are all present in pure lignin spectra and correlated with the AUR fraction (Table 2). However, the absorbances at 1512, and 1601 cm^{-1}, previously assigned to lignin (Xu et al. 2013), did not correlate with the AUR fraction in months 12–24; suggesting that the AUR was a mixture of structures (Galletti et al. 1993).

While the initial litter decomposition phase (i.e., 0–12 months) showed the recalcitrance of aliphatic C–H and buildup of microbial biomass, FTIR spectroscopic changes after the first 12 months of decomposition were less intense and showed fluctuations in the aliphatic C–H bands. Aliphatic C–H bands, which resisted decomposition during the initial stages of decomposition declined in months 24–36, suggesting the eventual loss or decomposition of C–H rich cell wall material.

Lignin versus cellulose and non-structural components decomposition

Cellular polysaccharides and proteins of the non-structural fraction are generally considered to be inherently labile. For lignin poor litter such as big bluestem, it was predicted for them to be also largely bioavailable (Aber et al. 1990; Soong et al. 2015). Our results supported this hypothesis, but they also indicated that not all of these inherently labile fractions were bioavailable since some remained undecomposed after 2 years (Fig. 3a). Our results suggested that inherent chemical recalcitrance is only one of the mechanisms controlling the persistence of a compound, and that complexation with other organic structures may have significantly prevented decomposition of labile structures at later decomposition stages (Hedges and Keil 1995; Knicker and Hatcher 1997).

Plots of cellulose/lignin against time effectively displayed the two stage decomposition of cellulose and lignin (Supplementary Fig. 1). These ratios illustrated the co-dependence of lignin methoxy groups and cellulose during the second stage of the litter decomposition process. A possible reason for the relationship between cellulose and lignin is that cellulose was being incorporated into the lignin during the decomposition process (Kolodziejski et al. 1982; Talbot et al. 2011). A strong correlation between etherified ferulate

(the crosslinking molecule for lignin) and NDF has been observed for other grasses (Casler and Jung 2006), suggesting that as lignin enrichment occurs it is accompanied by an increase in etherified ferulate. In the FTIR spectra there was a similar increase in the ether absorbance for the first year (Fig. 4). The relative increase in etherified lignin suggested that more recalcitrant material (with a basic cellulose source incorporated into lignin) dominated in the decomposed litter residues, due to a higher importance of lignin linkages relative to cellulose. There was no apparent relationship between cellulose and hemicellulose regions in the NMR spectra or between lignin and hemicellulose regions with decomposition time, which was in agreement with our earlier assessment and the FTIR data.

Conclusions

In this study we utilized three commonly used methods to study chemical changes in big bluestem litter residue decomposition to almost complete mass loss (97 %) in a tallgrass prairie. The wet chemical fractionation method showed a decrease of 85 % in the most traditionally considered labile fractions (such as the operationally defined non-structural fraction), but did not accurately describe the initial litter structures. NMR and FTIR data indicated that the actual structures contained in the litter changed more subtly during the course of the decomposition process, with cellulose dominating throughout. Thus, wet chemistry-based data should be interpreted with caution and this approach, if used, should always be coupled with spectroscopic approaches. Interestingly, we noted a two-step decomposition process with all three methods. In the first stage (0–12 months) we observed a strong loss in non-structural components, cellulose and hemicellulose, with a subsequent increase in the amount of AUR/cutin in the litter. In the second stage (12–36 months) we noted that all of the main structural groups of the litter were lost at approximately the same rate. In particular, we observed a strong correlation between cellulose and lignin, possibly suggesting the incorporation of cellulosic type structures into lignin, rendering them insoluble (and possibly classified as AUR by wet chemical fractionation). We found that structural class was only a good indicator for preferential removal or preservation in the earliest stages of decomposition, after which lignin encrustment limited the decomposition rate of cellulose, and all components decomposed at similar rates. Our two stage decomposition model was driven primarily by the intrinsic three-dimensional structure of the original litter and found that only the most bioavailable groups were removed during early decomposition, after which decomposition proceeded via a non-selective process.

Acknowledgments

We would like to thank the Konza Prairie LTER and EcoCore laboratories for their support and use of their facilities. The work was funded by the National Science Foundation (NSF)—Division of Environmental Biology grant #0918482, the NSF Graduate Research Fellowship Program, the United

States Department of Agriculture National Institute of Food and Agriculture, Agriculture and Food Research Initiative postdoctoral fellowship grant # 2012-01330, and the Cotrufo-Hoppess fund for soil ecology research. The wet chemical work was carried out at the EcoCore analytical services facility at Colorado State University (http://ecocore.nrel.colostate.edu/) with the help of Dr Liping Qiu. A portion of the research was performed using EMSL, a DOE Office of Science User Facility sponsored by the Office of Biological and Environmental Research and located at Pacific Northwest National Laboratory. We would like to thank the scientists at EMSL who assisted in running the NMR samples, particularly Dr. Sarah Burton.

References

Aber JD, Melillo JM, McClaugherty CA (1990) Predicting long-term patterns of mass loss, nitrogen dynamics, and soil organic matter formation from initial fine litter chemistry in temperate forest ecosystems. Can J Bot 68:2201–2208

Adair EC, Parton WJ, Del Grosso SJ et al (2008) Simple three-pool model accurately describes patterns of long-term litter decomposition in diverse climates. Glob Chang Biol 14:2636–2660. doi: 10.1111/j.1365-2486.2008.01674.x

Allen SE (1989) Chemical analysis of ecological materials. Blackwell, Oxford

Banerjee S, Li D (1991) Interpreting multicomponent infrared spectra by derivative minimization. Appl Spectrosc 45:1047–1049

Berg B, McClaugherty C (2007) Plant litter: decomposition, humus formation, carbon sequestration. Springer, Berlin

Berg B, Staaf H (1980) Decomposition rate and chemical changes of Scots pine needle litter. II. Influence of chemical composition. Ecol Bull 32:373–390

Bonanomi G, Incerti G, Giannino F et al (2013) Litter quality assessed by solid state ^{13}C NMR spectroscopy predicts decay rate better than C/N and Lignin/N ratios. Soil Biol Biochem 56:40–48. doi: 10.1016/j.soilbio.2012.03.003

Buxton DR, Russell JR (1988) Lignin constituents and cell-wall digestibility of grass and legume stems. Crop Sci 28:553–558

Calderón FJ, McCarty GW, Reeves JB (2006) Pyrolisis-MS and FT-IR analysis of fresh and decomposed dairy manure. J Anal Appl Pyrolysis 76:14–23. doi: 10.1016/j.jaap.2005.06.009

Calderón F, Haddix M, Conant R et al (2013) Diffuse-reflectance Fourier-transform mid-infrared spectroscopy as a method of characterizing changes in soil organic matter. Soil Sci Soc Am J 77:1591–1600. doi: 10.2136/sssaj2013.04.0131

Casler MD, Jung HG (1999) Selection and evaluation of smooth bromegrass clones with divergent lignin or etherified ferulic acid concentration. Crop Sci 39:1866–1873

Casler MD, Jung H-JG (2006) Relationships of fibre, lignin, and phenolics to in vitro fibre digestibility in three perennial grasses. Anim Feed Sci Technol 125:151–161. doi: 10.1016/j.anifeedsci.2005.05.015

Cortez J, Demard JM, Bottner P, Jocteur Monrozier L (1996) Decomposition of mediterranean leaf litters: a microcosm experiment investigating relationships between decomposition rates and litter quality. Soil Biol Biochem 28:443–452

Cotrufo MF, Soong JL, Horton AJ et al (2015) Formation of soil organic matter via biochemical and physical pathways of litter mass loss. Nat Geosci 8:776–779. doi: 10.1038/ngeo2520

Coûteaux M-M, Bottner P, Berg B (1995) Litter decomposition, climate and litter quality. Tree 10:63–66

Dann HM, Grant RJ, Van Amburgh ME, Van Soest PJ (2006) Lignin-carbohydrate linkages, lignin and the relationship with fiber digestibility. In: New York State College of Agriculture, and the Graduate School of Nutrition CU (ed) Proceedings of Cornell nutritive conference for feed manufacture, New York State College of Agriculture, and the Graduate School of Nutrition. Departments of Poultry Husbandry, Animal Husbandry, and Biochemistry and Nutrition, Cornell University, pp 87–98

Davies LM, Harris PJ, Newman RH (2002) Molecular ordering of cellulose after extraction of polysaccharides from primary cell walls of *Arabidopsis thaliana*: a solid-state CP/MAS 13C NMR study. Carbohydr Res 337:587–593

Galletti GC, Reeves JB III, Bloomfield J, Vogt KA, Vogt DJ (1993) Analysis of leaf and fine root litter from a subtropical montane rain forest by pyrolysis-gas chromatography/mass-spectrometry. J Anal Appl Pyrol 27:1–14

Goff BM, Murphy PT, Moore KJ (2012) Comparison of common lignin methods and modifications on forage and lignocellulosic biomass materials. J Sci Food Agric 92:751–758. doi: 10.1002/jsfa.4637

Gorgulu ST, Dogan M, Severcan F (2007) The characterization and differentiation of higher plants by fourier transform infrared spectroscopy. Appl Spectrosc 61:300–308. doi: 10.1366/000370207780220903

Haberhauer G, Gerzabek MH (1999) Drift and transmission FT-IR spectroscopy of forest soils: an approach to determine decomposition processes of forest litter. Vib Spectrosc 19:413–417. doi: 10.1016/S0924-2031(98)00046-0

Hamadi Z, Steinberger Y, Kutiel P et al (2000) Decomposition of *Avena sterilis* litter under arid conditions. J Arid Environ 46:281–293. doi: 10.1006/jare.2000.0672

Hedges JI, Keil RG (1995) Sedimentary organic matter preservation: an assessment and speculative synthesis. Mar Chem 49:81–115. doi: 10.1016/0304-4203(95)00008-F

Himmelsbach DS, Barton FE II, Windham WR (1983) Comparison of carbohydrate, lignin, and protein ratios between grass species by cross polarization-magic angle spinning carbon-13 nuclear magnetic resonance. J Agric Food Chem 31:401–404

Hindrichsen IK, Kreuzer M, Madsen J, Bach Knudsen KE (2006) Fiber and lignin analysis in concentrate, forage, and feces: detergent versus enzymatic-chemical method. J Dairy Sci 89:2168–2176. doi: 10.3168/jds.S0022-0302(06)72287-1

Ishler V, Varga G (2001) Carbohydrate nutrition for lactating dairy cattle. Pennsylvania State University, University Park, PA

Jung HG, Vogel KP (1992) Lignification of switchgrass (*Panicum virgatum*) and big bluestem (*Andropogon gerardii*) plant parts during maturation and its effect on fibre degradability. J Sci Food Agric 59:169–176

Kelleher BP, Simpson MJ, Simpson AJ (2006) Assessing the fate and transformation of plant residues in the terrestrial environment using HR-MAS NMR spectroscopy. Geochim Cosmochim Acta 70:4080–4094. doi: 10.1016/j.gca.2006.06.012

Klotzbücher T, Kaiser K, Guggenberger G et al (2011) A new conceptual model for the fate of lignin in decomposing plant litter. Ecology 92:1052–1062

Knapp AK, Briggs JM, Hartnett DC, Collins SL (1998) Grassland dynamics: long-term ecological research in tallgrass prairie. The Long-term ecological research network series, 1st edn. Oxford University Press, Oxford

Knicker H, Hatcher PG (1997) Survival of protein in an organic-rich sediment: possible protection by encapsulation in organic matter. Naturwissenschaften 84:231–234. doi: 10.1007/s001140050384

Kögel-Knabner I (2002) The macromolecular organic composition of plant and microbial residues as inputs to soil organic matter. Soil Biol Biochem 34:139–162

Kolodziejski W, Frye JS, Maclel GE (1982) Carbon-13 nuclear magnetic resonance spectrometry with cross polarization and magic-angle spinning for analysis of Lodgepole pine wood. Anal Chem 54:1419–1424

Lapierre C (1993) Application of new methods for the investigation of lignin structure. Forge cell wall structure and digestibility. ASA-CSSA-SSSA, Madison, pp 133–166

Lewis NG, Razal RA, Dhara KP et al (1988) Incorporation of [2-^{13}C] ferulic acid, a lignin precursor, into *Leucaena leucocephala* and its analysis by solid state ^{13}C N.M.R spectroscopy. J Chem Soc, Chem Commun. doi: 10.1039/C39880001626

Lorenz K, Preston CM, Krumrei S, Feger K-H (2004) Decomposition of needle/leaf litter from Scots pine, black cherry, common oak and European

beech at a conurbation forest site. Eur J For Res 123:177–188. doi: 10.1007/s10342-004-0025-7

Madejová J, Kečkés J, Pálková H, Komadel P (2002) Identification of components in smectite/kaolinite mixtures. Clay Miner 37:377–388. doi: 10.1180/0009855023720042

Mascarenhas M, Dighton J, Arbuckle GA (2000) Characterization of plant carbohydrates and changes in leaf carbohydrate chemistry due to chemical and enzymatic degradation measured by microscopic ATR FT-IR spectroscopy. Appl Spectrosc 54:681–686. doi: 10.1366/0003702001950166

Nelson PN, Baldock JA (2005) Estimating the molecular composition of a diverse range of natural organic materials from solid-state ^{13}C NMR and elemental analyses. Biogeochemistry 72:1–34. doi: 10.1007/s10533-004-0076-3

Nguyen TT, Janik LJ, Raupach M (1991) Diffuse reflectance infrared Fourier transform (DRIFT) spectroscopy in soil studies. Aust J Soil Res 29:49–67

Nikonenko NA, Buslov DK, Sushko NI, Zhbankov RG (2005) Spectroscopic manifestation of stretching vibrations of glycosidic linkage in polysaccharides. J Mol Struct 752:20–24. doi: 10.1016/j.molstruc.2005.05.015

Nordén B, Berg B (1990) A non-destructive method (solid state ^{13}C NMR) for determining organic chemical components of decomposing litter. Soil Biol Biochem 22:271–275

Preston CM, Trofymow JA, Sayer BG, Niu J (1997) ^{13}C nuclear magnetic resonance spectroscopy with cross-polarization and magic-angle spinning investigation of the proximate-analysis fractions used to assess litter quality in decomposition studies. Can J Bot 75:1601–1613

Preston CM, Nault JR, Trofymow JA (2009) Chemical changes during 6 years of decomposition of 11 litters in some Canadian sites. Part 2. ^{13}C abundance, solid-state 13C NMR spectroscopy and the meaning of “Lignin”. Ecosystems 12:1078–1102. doi: 10.1007/sl0021-009-9267-z

Reeves JB, McCarty GW, Rutherford DW, Wershaw RL (2008) Mid-infrared diffuse reflectance spectroscopic examination of charred pine wood, bark, cellulose, and lignin: implications for the quantitative determination of charcoal in soils. Appl Spectrosc 62:182–189. doi: 10.1366/000370208783575618

Rovira P, Rovira R (2010) Fitting litter decomposition datasets to mathematical curves: towards a generalised exponential approach. Geoderma 155:329–343. doi: 10.1016/j.geoderma.2009.11.033

Rowland AP, Roberts JD (1994) Lignin and cellulose fractionation in decomposition studies using acid-detergent fibre methods. Commun Soil Sci Plant Anal 25:269–277

Rumpel C, Eusterhues K, Kögel-Knabner I (2004) Location and chemical composition of stabilized organic carbon in topsoil and subsoil horizons of two acid forest soils. Soil Biol Biochem 36:177–190. doi: 10.1016/j.soilbio.2003.09.005

Sariyildiz T, Anderson JM (2003) Interactions between litter quality, decomposition and soil fertility: a laboratory study. Soil Biol Biochem 35:391–399. doi: 10.1016/S0038-0717(02)00290-0

Sjöberg G, Nilsson SI, Persson T, Karlsson P (2004) Degradation of hemicellulose, cellulose and lignin in decomposing spruce needle litter in relation to N. Soil Biol Biochem 36:1761–1768. doi: 10.1016/j.soilbio.2004.03.010

Sluiter JB, Ruiz RO, Scarlata CJ et al (2010) Compositional analysis of lignocellulosic feedstocks. 1. Review and description of methods. J Agric Food Chem 58:9043–9053. doi: 10.1021/jf1008023

Smith BC (2011) Fundamentals of Fourier transform infrared spectroscopy, 2nd edn. CRC Press

Socrates G (1994) Infrared characteristic group frequencies, 2nd edn. Wiley, West Sussex

Soong JL, Calderón FJ, Betzen J, Cotrufo MF (2014a) Quantification and FTIR characterization of dissolved organic carbon and total dissolved nitrogen leached from litter: a comparison of methods across litter types. Plant Soil 385:125–137. doi: 10.1007/s11104-014-2232-4

Soong JL, Reuss D, Pinney C et al (2014b) Design and operation of a continuous ^{13}C and ^{15}N labeling chamber for uniform or differential, metabolic and structural, plant isotope labeling. J Vis Exp 83:e51117. doi: 10.3791/51117

Soong JL, Parton W, Calderón F et al (2015) A new conceptual model on the fate and controls of fresh and pyrolized plant litter decomposition. Biogeochemistry 8:776–779. doi: 10.1007/s10533-015-0079-2

Soong JL, Vandegehuchte ML, Horton AJ et al (2016) Soil microarthropods support ecosystem productivity and soil C accrual: evidence from a litter decomposition study in the tallgrass prairie. Soil Biol Biochem 92:230–238. doi: 10.1016/j.soilbio.2015.10.014

Spence A, Simpson AJ, McNally DJ et al (2011) The degradation characteristics of microbial biomass in soil. Geochim Cosmochim Acta 75:2571–2581. doi: 10.1016/j.gca.2011.03.012

Spielvogel S, Prietzel J, Kögel-Knabner I et al (2010) Lignin phenols and cutin- and suberin-derived aliphatic monomers as biomarkers for stand history. Geochim Cosmochim Acta 74:A983–A983

Stewart D, Mcdougall GJ, Baty A (1995) Fourier-transform infrared microspectroscopy of anatomically different cells of flax (*Linum usitatissimum*) stems during development. J Agric Food Chem 43:1853–1858

Talbot JM, Yelle DJ, Nowick J, Treseder KK (2011) Litter decay rates are determined by lignin chemistry. Biogeochemistry 108:279–295. doi: 10.1007/s10533-011-9599-6

Theerarattananoon K, Xu F, Wilson J et al (2012) Impact of pelleting and acid pretreatment on biomass structure and thermal properties of wheat straw, corn stover, blue bluestem, and sorghum stalk. Trans ASABE 55:1845–1858

Tremblay L, Gagne JP (2002) Fast quantification of humic substances and organic matter by direct analysis of sediments using DRIFT spectroscopy. Anal Chem 74:2985–2993

Udén P, Robinson PH, Wiseman J (2005) Use of detergent system terminology and criteria for submission of manuscripts on new, or revised, analytical methods as well as descriptive information on feed analysis and/or variability. Anim Feed Sci Technol 118:181–186. doi: 10.1016/j.anifeedsci.2004.11.011

Van Soest PJ, Wine RH (1967) Use of detergents in the analysis of fibrous feeds. IV. Determination of plant cell-wall constituents. J Assoc Off Anal Chem 46:50–55

Van Soest PJ, Wine RH (1968) Determination of lignin and cellulose in acid-detergent fiber with permanganate. J Assoc Off Anal Chem 51:780–785

Van Soest PJ, Robertson JB, Lewis BA (1991) Methods for dietary fiber, neutral detergent fiber, and nonstarch polysaccharides in relation to animal nutrition. J Dairy Sci 74:3583–3597

Vanderhart DL, Atalla RH (1984) Studies of microstructure in native celluloses using solid-state ^{13}C NMR. Macromolecules 17:1465–1472

Whitbeck MR (1981) Second derivative infrared spectroscopy. Appl Spectrosc 35:93–95

Xu F, Yu J, Tesso T et al (2013) Qualitative and quantitative analysis of lignocellulosic biomass using infrared techniques: a mini-review. Appl Energy 104:801–809

Zhang K, Johnson L, Nelson R et al (2012) Chemical and elemental composition of big bluestem as affected by ecotype and planting location along the precipitation gradient of the Great Plains. Ind Crops Prod 40:210–218. doi: 10.1016/j.indcrop.2012.03.016